The Journal of Chemical Physics

Dynamic and stress signatures of the rigid intermediate phase in glass-forming liquids

Cite as: J. Chem. Phys. **152**, 221101 (2020); https://doi.org/10.1063/5.0007093
Submitted: 17 March 2020 . Accepted: 27 May 2020 . Published Online: 11 June 2020

W. Song, X. Li, M. Wang, M. Bauchy, and M. Micoulaut

The Journal of Chemical Physics COMMUNICATION scitation.org/journal/jcp

Dynamic and stress signatures of the rigid intermediate phase in glass-forming liquids

Cite as: J. Chem. Phys. 152, 221101 (2020); doi: 10.1063/5.0007093
Submitted: 17 March 2020 • Accepted: 27 May 2020 •
Published Online: 11 June 2020

W. Song,[1] X. Li,[1] M. Wang,[1,2] M. Bauchy,[1] and M. Micoulaut[3,a)]

AFFILIATIONS

[1]Physics of AmoRphous and Inorganic Solids Laboratory (PARISlab), Department of Civil and Environmental Engineering, University of California, Los Angeles, California 90095, USA
[2]Department of Materials Science and Engineering, Massachusetts Institute of Technology, Cambridge, Massachusetts 02139, USA
[3]Sorbonne Université, Laboratoire de Physique Théorique de la Matière Condensée, 4 Place Jussieu, F-75252 Paris Cedex 05, France

[a)]**Author to whom correspondence should be addressed:** mmi@lptmc.jussieu.fr

ABSTRACT

We study the evolution of enthalpic changes across the glass transition of model sodium silicate glasses $(Na_2O)_x(SiO_2)_{100-x}$, focusing on the detection of a flexible-rigid transition and a possible reversibility window in relationship with dynamic properties. We show that the hysteresis resulting from enthalpic relaxation during a numerical cooling–heating cycle is minimized for $12\% \le x \le 20\%$ Na_2O, which echoes with the experimental observation. The key result is the identification of the physical features driving this anomalous behavior. The intermediate-flexible boundary is associated with a dynamic onset with increasing depolymerization that enhances the growing atomic motion with a reduced internal stress, whereas the intermediate-stressed rigid boundary exhibits a substantial increase in the temperature at which the relaxation is maximum. These results suggest an essentially dynamic origin for the intermediate phase observed in network glass-forming liquids.

There are many disordered systems that can be modeled as topological networks with varying connectedness, e.g., glasses, liquids, packings of particles, or insulators. In order to predict the physical behavior, an interesting means builds on the notion of Maxwell–Lagrange rigidity, which has the advantage to simplify the description of such complex systems via the enumeration of interactions (or topological constraint density n_c) and degrees of freedom.[1,2] When applied to glasses, the mean-field Phillips–Thorpe (MFPT) treatment[1] predicts that an amorphous network will progressively stiffen and become rigid at the atomic scale (i.e., local deformation modes) when the connectivity or network mean coordination number $\bar{r}$ increases. This has led to the recognition of a rigidity transition[3] separating an underconstrained phase (or flexible phase, when $n_c < 3$) from an overconstrained phase (or stressed-rigid phase, when $n_c > 3$).

The key feature of the MFPT theory is a solitary transition at $n_c = 3$ occurring at some critical coordination number $\bar{r}_c$ that coincides with the location of the Maxwell stability criterion for isostatic structures (i.e., when densities of constraints and degrees of freedom match with each other). Numerous experiments have confirmed these simple predictions in glasses, liquids, or even polymers[4] but have also revealed that there is a range of "equivalent" compositions (or coordination numbers) for which the corresponding supercooled liquid is strong[5] and where the glass displays space-filling tendencies[6] and reduced aging phenomena.[7] In addition, enthalpic changes are extraordinarily small across the glass transition for such compositions, and hence, these define a reversibility window (RW) in calorimetric experiments[8,9] that appear to be linked not only with properties of the corresponding supercooled liquids such as the fragility or ease of relaxation[5,10] but also with properties of the glassy state such as the structure or molar volume.[11] Idealized bond depleted networks at zero temperature[12,13] or toy models[14–17] suggest that RWs are the signature of an intermediate phase found between the flexible and stressed-rigid phases. However, while such results represent an interesting step forward for an increased understanding, the physics of RWs remains to be characterized.

In the present Communication, we investigate from molecular dynamics (MD) simulations a realistic network structure with varying connectivity subject to both thermal changes and associated relaxation during glass formation. A reversibility window is obtained at the glass transition that is compatible with experimental observations. We show that the intermediate-flexible boundary is linked with the presence of a dynamical threshold that promotes atomic motion in the flexible phase and identify the networks of the RW to be isostatic in character but with a marked growth in internal stress. While the physics of intermediate phases is fully characterized on idealized networks at zero temperature from a double percolative transition, rigidity, and stress, for real amorphous materials at finite temperature with a true physical interaction and subject to glassy relaxation, complexity emerges so that the obtained signatures contain only the fingerprints of the $T = 0$ behavior.

The model and framework used to reach the conclusions presented herein build on a recently introduced methodology that relies on numerical cooling–heating cycles across the glass transition.[18] A series of sodium silicate glasses $(Na_2O)_x(SiO_2)_{100-x}$ ranging from $x = 0$ (silica) to 40% Na_2O with 3000 atoms are simulated with an integration time step of 1 fs. We adopt the well-established Teter potential,[19] with a short-range interaction cutoff taken as 8.0 Å and the Coulomb interactions being evaluated by the Ewald summation method with a cutoff of 12 Å. The validity of this potential has been extensively verified in the liquid and glassy phases for different compositions.[19–21] The glass samples are first equilibrated in the liquid state (4000 K, zero pressure, *NPT* ensemble) to ensure the loss of the memory of the initial configuration. It should be noted that prior to the present work, extended investigations have been performed on this system under various thermodynamic conditions (NPT, NVT, cooling rate, etc.) but for a single composition only (x = 33%).[22–25] Each system is then subjected to a thermal cycle (cooling followed by subsequent reheating) with cooling and heating rates fixed at 1 K/ps under zero pressure in the *NPT* ensemble (Fig. 1). During the course of the cycle, prior to each temperature increment, 16 configurations are extracted and subjected to an energy minimization in order to access the enthalpy of the inherent configuration as a function of temperature, as averaged over the 16 configurations.[18] Last but not least, each thermal simulation is repeated six times so that the analyzed enthalpy relaxation during the cycle is the result of an average over six repetitions. Figure 1 shows an example of such an averaged thermal cycle. The enthalpy reported is one of the inherent structures which permits to filter out thermal effects given that it removes contributions arising from thermal fluctuations of the atoms around their local (metastable) equilibrium position.

As expected, in most of the situations and as in Fig. 1, the glass transition is not reversible, that is, the cooling and heating curves do not exactly overlap. This non-reversibility manifests itself by a hysteresis cycle, which is simply the result of the enthalpic relaxation in the vicinity of the glass transition and an indication of the out-of-equilibrium nature of the glassy state. Indeed, visible relaxation effects only occur close to the fictive temperature (here, $T_f \simeq 2500$ K), whereas the system equilibrates rather easily on short time scales at high-temperature. Following Ref. 18, in order to quantify the extent of enthalpy relaxation, we fit the difference of enthalpy during cooling and reheating [$\Delta H(T)$; see the inset of Fig. 1] by a Gaussian function $\Delta H(T) = \Delta H_{\max} \exp[-(T - T_{\max})^2/2\sigma_T^2]$, where

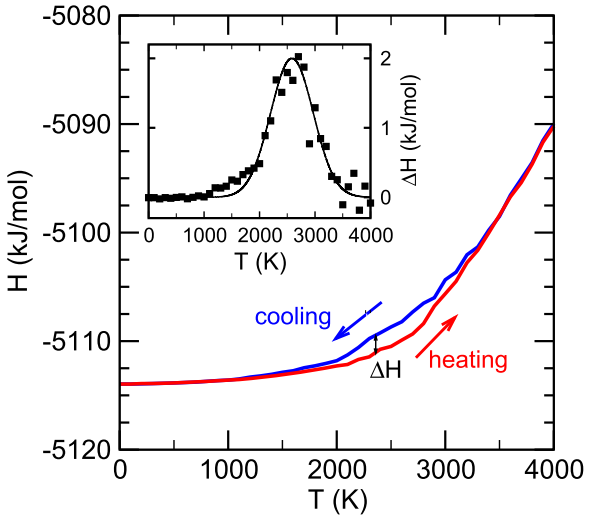

FIG. 1. Ground-state enthalpy (H) in a $(Na_2O)_5(SiO_2)_{95}$ glass as a function of temperature during a thermal cycle (cooling followed by reheating). The inset shows the difference in enthalpy (ΔH) upon cooling and reheating as a function of temperature. The solid line is the Gaussian fit (see text for details).

$\Delta H_{\max}$ corresponds to the maximum extent of the relaxation, $T_{\max}$ is the temperature at which enthalpy relaxation is maximum, and σ_T is related to the width of the range of temperature over which relaxation occurs.

The effect of the glass composition on $\Delta H_{\max}$ and $T_{\max}$ is represented in Fig. 2. We find that the maximum extent of enthalpy relaxation $\Delta H_{\max}$ displays a global decrease with increasing sodium content, but, interestingly, with a marked minimum between $x = 12\%$ and 20%, which is indicative of a reversibility window as $\Delta H_{\max}$ is found to decrease by nearly 25% within this composition interval. In similar systems under pressure, such RWs have been found to not depend on the applied cooling/heating rate[22] and, thereby, appear to be an intrinsic property of the material. The observation is, furthermore, directly comparable with the results from modulated differential calorimetry on sodium silicate glasses,[26] which revealed a similar RW at a somewhat higher soda composition (18%–22%). The temperature of maximum relaxation $T_{\max}$ exhibits a decrease with the modifier content (the inset of Fig. 2) in qualitative agreement with the fact that the glass transition temperature T_g decreases with increasing x.[26] This arises from the fact that the system becomes more and more depolymerized, and hence, its viscosity decreases so that its freezing point shifts toward lower temperature. However, $T_{\max}$ displays two marked regimes as $T_{\max}$ decreases substantially up to 19% Na_2O (with a slope of −10.61 K mol^{-1}), then, exhibits a clear break in slope with further changes, and evolves at a smaller rate (with a slope of −5.87 K mol^{-1}), the locus of this transition/threshold being obviously linked with the sodium-rich boundary of the RW.

We now investigate from the MD network structure how the atomic topology and rigidity control the propensity for glass transition reversibility. We use a recent MD-based constraint counting algorithm to estimate the constraint density n_c, which consists in

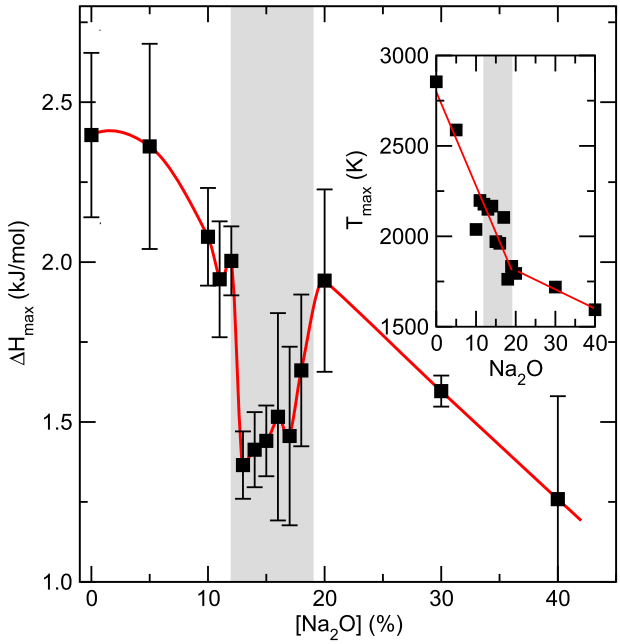

FIG. 2. Maximum extent of relaxation (ΔH_{max}) at T_{max} as a function of composition (Na_2O) in Na_2O–SiO_2 glasses. Error bars represent the standard deviations over the six repetitions. The inset shows the temperature at which relaxation is maximum (T_{max}). The approximate gray zone is defined from the drop of ΔH_{max}.

computing the radial and angular excursion of the neighbors of each atom to infer the number of active bond-stretching and bond-bending constraints.[2,23] Here, the numerical results for n_c are found to behave exactly according to the MFPT estimate[3] $n_c = \frac{1}{3}[11 - 10x]$, which assumes the effective coordination numbers r for Si, O, and Na to be, respectively, 4, 2, and 1.[23] The estimate is established by assuming that $(2r - 3)$ angular and $r/2$ radial interactions constrain the system at the atomic level. According to Ref. 26, the present silicate $Si_{1-x}O_{2-x}Na_{2x}$ also contains NBO atoms whose Si–NBO–Na angular interactions become ineffective in the presence of the sodium atoms[23] so that one may write $Si_{1-x}(BO)_{2-3x}(NBO)_{2x}Na_{2x}$. This leads to an estimate of $(7 - 7x)$, $(4 - 6x)$, $2x$, and x for Si, BO, NBO, and Na, respectively, and a special care has to be taken into account for the one-fold Na atoms.[27] Taken together, one has $11 - 10x$ constraints per formula unit, and this yields an isostatic Maxwell stability criterion at $x = 20\%$, which is compatible with the present results.

Results of ΔH_{max} (Fig. 2) are now represented as a function of the constraint density n_c computed in the glass [Fig. 3(a)]. This reveals that, close to $n_c = 3$ (i.e., $x = 20\%$ Na_2O), glasses undergo a glass transition with minimal enthalpic changes, which is a characteristic of an RW. The extent of the RW from roughly $n_c = 3.0$ to 3.3 has been acknowledged in chalcogenide systems, where the octet rule permits to rigorously link n_c with glass composition.[27] Conversely, stressed-rigid systems ($n_c > 3$) at higher silica content and the flexible ($n_c < 3$) ones at higher sodium content induce a larger extent of relaxation that manifests in a larger value for ΔH_{max}. The physical origin of this trend can now be clarified, and this provides

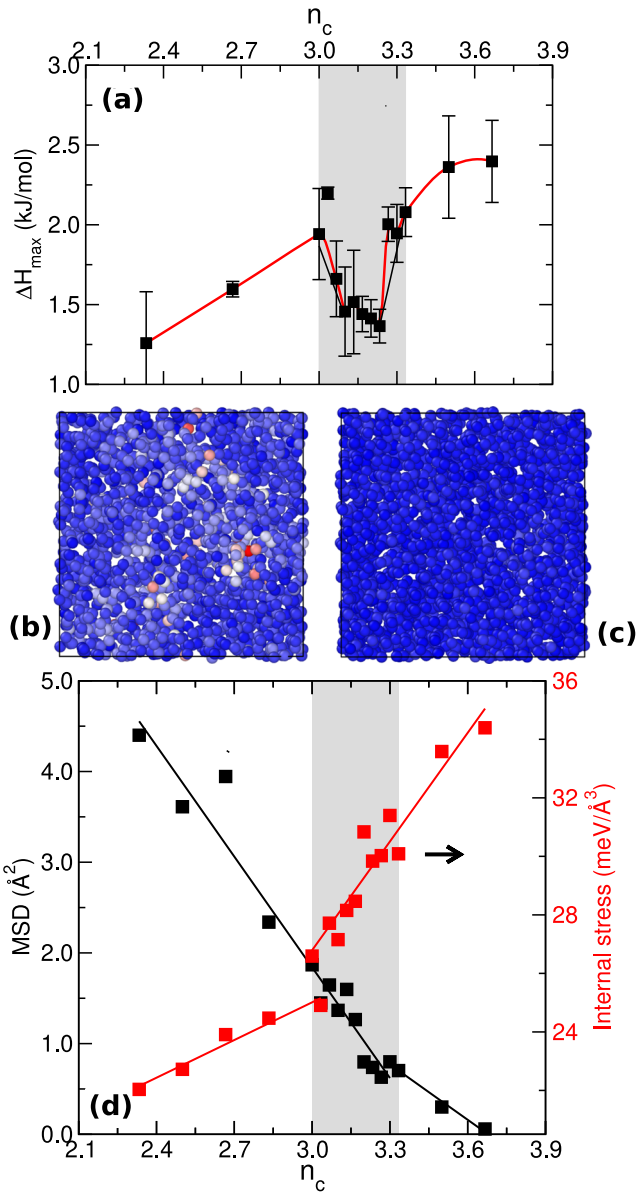

FIG. 3. (a) Maximum extent of relaxation (ΔH_{max}, the same as Fig. 2) at T_{max} as a function of the constraint density n_c in Na_2O–SiO_2 glasses. Atomic snapshots for $n_c = 2.3$ (b) and $n_c = 3.66$ (c) are colored according to the calculated MSD per atom. (d) Atomic mean square displacement (MSD) at 300 K (left axis, black symbols) and internal stress (right axis, red symbols) as a function of n_c.

an additional insight that has not been considered before. Stressed-rigid materials display an intrinsically large bond density, which induces some stress (i.e., $n_c - 3$[14]) that prevents from a full relaxation of the enthalpy during cooling. This situation is also met for flexible glasses, which continue to relax at low temperature due to the presence of low frequency modes (i.e., $3 - n_c$[28]). At some more balanced compositions (close to the isostatic threshold), such modes tend to reduce substantially and their density becomes strictly zero

at $x = 20\%$ in the MFPT picture. These balanced (and nearly isostatic) compositions also contain a smaller fraction of bonds, which reduces the possibility to have stress relaxation.

In order to measure the degree of stress acting in the atomic network, we rely on the concept of "*stress per atom*." Although stress can only be meaningfully defined at the macroscopic scale, we adopt here the formalism proposed by Thompson *et al.*,[29] which expresses the contribution of each atom to the virial of the system. By using a Voronoi tessellation to define the volume of an atom, its local "pressure" is then defined as the trace of the calculated local stress tensor. Note that, although the network as a whole is at zero pressure, some bonds are under compression while others are under tension so that they mutually compensate each other. We then focus on bridging oxygen (BO) atoms, that is, atoms which are connected to two Si atoms and contribute mostly to the connectivity of the rigid backbone. To isolate the contribution of the network to the stress of each BO, the "*stress per atom*" calculation is repeated on an isolated Q^1–Q^1 "*dimer*" cluster containing a single BO.[30] Finally, the *internal stress* of each BO in the glass is calculated from the difference $\Delta\sigma$ between its states of stress in the network and isolated cluster, which corresponds to the network stress, that is, the stress imposed on the BO atoms by the increasing network connectivity between SiO_4 polytopes.[31] One should also have in mind that in contrast to the strong ionocovalent Si–O bonds, Na–O bonds involving NBO's are more ionic and significantly weaker. Hence, they do not contribute to carrying any stress throughout the network (which is concentrated within the strong silicate skeleton of the glass), and our stress/atom analysis does not reveal any notable internal stress for such NBO atoms, as also recently revealed.[37]

Once represented as a function of n_c [Fig. 3(d), right axis], one realizes, indeed, that a substantial increase in $\Delta\sigma$ is obtained for $n_c > 3$ with a possible jump at the flexible-intermediate boundary although the large fluctuations prevent us from ensuring that this might be a first-order transition, as suggested from simple bar networks at zero temperature.[12]

In addition, we note that the atomic mobility (AM) also indicates a marked change in behavior close to the RW compositions. Such an AM is obtained here by applying an instantaneous energy bump of 0.2 eV/atom to the 0 K inherent configuration of the glass.[32] The energy is here chosen to be high enough to allow potential motion between low energy barriers but low enough to avoid any glass transition or melting of the system. The system is then allowed to evolve in the microcanonical ensemble (*NVE*) for 100 ps during which the mean square displacement (MSD) of the atoms is computed. Figure 3(d) now indicates that flexible compositions ($n_c < 3$) will permit an enhanced atomic motion given the presence of a larger number of energy channels in the potential energy landscape.[33] It is furthermore noted that this motion is heterogeneous in character [Fig. 3(d)], as reminiscent of the critical behavior in the liquid state.[34]

The outcome that emerges from this study indicates a more complex physical picture of intermediate phases involving obvious contributions arising from kinetics and thermodynamics. Weakly connected glasses having either a chain-like structure (e.g., chalcogen-rich systems as $Ge_{10}Se_{90}$) or a depolymerized network (e.g., sodium-rich silicates or phosphates) are flexible ($n_c < 3$) and exhibit a noticeable increase in atomic mobility that manifests not only by a large MSD but also an enhanced diffusivity in the liquid state.[35] This suggests that, in flexible glasses, relaxation is kinetically favored by the fact that the atoms have a high mobility. This also induces the possibility of glassy relaxation that gives rise to more pronounced enthalpic changes during a cooling/heating cycle. In contrast, stressed-rigid glasses ($n_c > 3$) that correspond to usual stoichiometric compounds (e.g., $SiSe_2$, GeO_2, etc.) or network-former-rich modified glasses exhibit a low atomic mobility, but present some internal stress at the atomic scale. This signals that the network is locally unstable and acts as an energy penalty (driving force) that enhances the propensity for relaxation. This suggests that, in stressed-rigid glasses, relaxation is thermodynamically driven. Overall, isostatic glasses exhibit minimum relaxation as they feature an optimal balance between low atomic mobility and limited internal stress. In this respect, it is interesting to note that the experimental locus of RWs often coincides with minima in activation barriers for enthalpic or viscous relaxation.[5,20] In addition, for this particular binary system, it is important to realize that the compositions belonging to the stressed rigid phase ($x < 12\%$) merely coincide with those displaying immiscibility,[36] and it is tempting to relate both phenomena as it is the case at the nanoscale for certain chalcogenides.[37] We hypothesize that the existence of internal stress in the network could act as an energy penalty promoting phase separation.

In summary, we rationalize these two threshold compositions at 12% and 19% as follows. For $x > 19\%$ ($n_c < 3$), the glass is atomically flexible based on the mean-field enumeration of the topological constraints. In this regime, atomic mobility is high and the network does not exhibit any significant internal stress [Fig. 3(d)]. In this regime, the network is macroscopically flexible. At $x = 19\%$, however, corresponding to $n_c \simeq 3$, the system exhibits a macroscopic percolation of rigidity throughout its network, which results in the formation of some stress within the structure. Nevertheless, at this threshold, the glass still exhibits some local flexibility since the MSD after an energy bump remains non-negligible. Here, both the temperature at which relaxation is maximum and the internal stress acting within the network exhibit a sudden increase. With decreasing modifier composition, the MSD eventually drops to about 0.5 Å^2 at $x = 12\%$. This defines a second region ($12\% < x < 19\%$) wherein the network is macroscopically rigid (as evidenced by the existence of internal stress), but, locally, still exhibits some localized floppy modes that permit some atomic motion. Finally, at $x < 12\%$ ($n_c > 3.3$), the system does not exhibit any notable internal flexibility any longer and the MSD becomes negligible [Fig. 3(d)], which indicates a fully locked atomic structure with stressed-rigid domains. At this point, the network is rigid both at the macroscopic and local scales.

Altogether, the present results on an archetypal glass system highlight the existence of special compositions having some optimal connectivity, which underscores the strong relationship between atomic topology and relaxation events occurring during the glass transition. These numerical results provide a strong support to the experimental signature of RWs[8,9,26] and signal rapid changes in dynamic properties and stress, these changes being revealed and analyzed here for the first time. From a more applied viewpoint, it is realized that the understanding and prediction of relaxation properties of glasses from such tools might be used to explore new compositional spaces using the very special properties of RW glasses.

This work was supported by the National Science Foundation under Grant No. 1928538 and by Corning Incorporated through the Glass Age Scholarship.

DATA AVAILABILITY

The data that support the findings of this study are available from the corresponding author upon reasonable request.

REFERENCES

[1] J. C. Phillips, J. Non-Cryst. Solids **34**, 153 (1979).
[2] M. Bauchy, Comput. Mater. Sci. **159**, 95 (2019).
[3] H. He and M. F. Thorpe, Phys. Rev. Lett. **54**, 2107 (1985).
[4] *Rigidity Theory and Applications*, edited by M. F. Thorpe and P. M. Duxburry (Plenum Press, Kluwer, NY, 1999).
[5] K. Gunasekara, S. Bhosle, P. Boolchand, and M. Micoulaut, J. Chem. Phys. **139**, 164511 (2013).
[6] C. Bourgel, M. Micoulaut, M. Malki, and P. Simon, Phys. Rev. B **79**, 024201 (2009).
[7] P. Chen, P. Boolchand, and D. G. Georgiev, J. Phys.: Condens. Matter **22**, 065104 (2010).
[8] D. Selvanathan, W. J. Bresser, and P. Boolchand, Phys. Rev. B **61**, 15061 (2000).
[9] P. Boolchand, P. Chen, and U. Vempati, J. Non-Cryst. Solids **355**, 1773 (2009).
[10] S. Ravindren, K. Gunasekera, Z. Tucker, A. Diebold, P. Boolchand, and M. Micoulaut, J. Chem. Phys. **140**, 134501 (2014).
[11] M. Micoulaut, Adv. Phys.: X **1**, 147 (2016).
[12] M. F. Thorpe, D. J. Jacobs, M. V. Chubynsky, and J. C. Phillips, J. Non-Cryst. Solids **266-269**, 859 (2000).
[13] M. Micoulaut, Phys. Rev. B **74**, 184208 (2006).
[14] J. Barré, A. R. Bishop, T. Lookman, and A. Saxena, Phys. Rev. Lett. **94**, 208701 (2005).
[15] M. V. Chubynsky, M.-A. Brière, and N. Mousseau, Phys. Rev. E **74**, 016116 (2006).
[16] L. Yan and M. Wyart, Phys. Rev. Lett. **113**, 215504 (2014).
[17] L. Yan, Nat. Commun. **9**, 1359 (2018).
[18] Z. Liu, Y. Hu, X. Li, W. Song, S. Goyal, M. Micoulaut, and M. Bauchy, Phys. Rev. B **98**, 104205 (2018).
[19] A. N. Cormack, J. Du, and T. R. Zeitler, J. Non-Cryst. Solids **323**, 147 (2003).
[20] M. Bauchy, B. Guillot, M. Micoulaut, and N. Sator, Chem. Geol. **346**, 47 (2013).
[21] J. Du and L. R. Corrales, Phys. Rev. B **72**, 092201 (2005).
[22] B. Mantisi, M. Bauchy, and M. Micoulaut, Phys. Rev. B **92**, 134201 (2015).
[23] M. Bauchy and M. Micoulaut, J. Non-Cryst. Solids **357**, 2530 (2011).
[24] M. Bauchy and M. Micoulaut, Nat. Commun. **6**, 6398 (2015).
[25] M. Bauchy, J. Chem. Phys. **137**, 044510 (2012).
[26] Y. Vaills, T. Qu, M. Micoulaut, F. Chaimbault, and P. Boolchand, J. Phys.: Condens. Matter **17**, 4889 (2005).
[27] M. Micoulaut, Rep. Prog. Phys. **79**, 066504 (2016).
[28] W. A. Kamitakahara, R. L. Cappelletti, P. Boolchand, B. Halfpap, F. Gompf, D. A. Neumann, and H. Mutka, Phys. Rev. B **44**, 94 (1991).
[29] A. P. Thompson, S. J. Plimpton, and W. Mattson, J. Chem. Phys. **131**, 154107 (2009).
[30] The so-called Q^1 species corresponds to a $Na_3SiO_{5/2}$ unit, which leaves only a single BO atom left in a Q^1–Q^1 "*dimer*".
[31] X. Li, W. Song, M. M. Smedskjaer, J. C. Mauro, and M. Bauchy, J. Non-Cryst. Solids: X **1**, 100013 (2019).
[32] N. M. A. Krishnan, B. Wang, Y. Yu, Y. Le Pape, G. Sant, and M. Bauchy, Phys. Rev. X **7**, 031019 (2017).
[33] G. G. Naumis, Phys. Rev. B **71**, 026114 (2005).
[34] M. Micoulaut and M. Bauchy, Phys. Rev. Lett. **118**, 145502 (2017).
[35] C. Yildirim, J.-Y. Raty, and M. Micoulaut, Nat. Commun. **7**, 11086 (2016).
[36] G. L. Hovis, M. J. Toplis, and P. Richet, Chem. Geol. **213**, 173 (2004).
[37] P. Boolchand, D. G. Georgiev, T. Qu, F. Wang, L. Cai, and S. Chakravarty, C. R. Chim. **5**, 713 (2002).